International Journal of Thermofluid Science and Technology (2021)
Volume 8, Issue 3, Paper No. 080302
https://doi.org/10.36963/IJTST.2021080302
Research Article

Magnetohydrodynamics Flow of Nanofluid past an Elongating Sheet with Exponential Space-Based Heat Source and Homogeneous-Heterogeneous Chemical Reactions

K. Swain*, M. Mishra, P. K. Rout

Department of Mathematics, Gandhi Institute for Technology, Bhubaneswar- 752054, Odisha, India

ATICLE INFO

Received: 20 April 2021;
Received in revised form:
29 June 2021;
Accepted: 12 July 2021;
Published online:
18 July 2021

Keywords:
Nanofluid
Thermal radiation
Exponential Space-based Heat Source/Sink
Homogeneous and Heterogeneous Chemical Reactions

ABSTRACT

The present article deals with the MHD nanofluid flow over an elongating sheet in a saturated porous matrix. Two different nanoparticles with water as base fluid is considered. Similarity transformations convert the governing partial differential equations (PDEs) into ordinary differential equations (ODEs) and are solved numerically by effective shooting technique. The influences of pertinent parameters relating to the flow problem such as magnetic parameter, porosity parameter, thermal radiation, exponential space-based heat source/sink and most importantly homogeneous-heterogeneous chemical reaction of reactive species on the nanofluid velocity, temperature, concentration as well as skin-friction coefficient and heat transfer coefficients are studied via graphs and table. It is found that heat transfer rate of $Cu-water$ is higher than that of $Al_2O_3-water$. Velocity of $Al_2O_3-water$ nanofluid is slightly on lower side as compared to $Cu-water$ nanofluid whereas reverse effect is observed in case of temperature profile.

1. Introduction

Numerous investigations were made on the flow and heat transfer over an elongating surface in different directions due to its wide applications in metallurgy, extrusion processes, food processing, movement of biological fluids, and glass fiber production etc. Nadeem et al. [1] examined the nanofluid flow over a stretching sheet. Gireesha et al. [2] analysed the heat and mass transfer of a chemically reacting Casson fluid over a permeable stretching surface. Das [3] studied the slip flow analysis of nanofluid flow over a non-linear permeable stretching sheet. Farooq et al. [4] established the series solutions of non-similarity boundary layer flow of nanofluids over widening surface. Rout and Mishra [5] examined the MHD nanofluid flow over an extending surface. Swain et al. [6] studied the MHD flow of viscoelastic nanofluid over a stretching sheet in a porous medium. Shankar Goud et al. [7] examined the unsteady free convection flow of viscous fluid past an exponentially accelerated inclined plate with variable temperature and thermal Radiation. Senapati et al. [8] numerically examined 3D flow of Casson fluid by taking

*Corresponding e-mail: kharabela1983@gmail.com (Kharabela Swain)

Nomenclature

a_0	Concentration of the foreign species	Q^*	Heat source/sink coefficient
B_0	Magnetic field strength	R	Radiation parameter
C_f	Local skin friction coefficient	Re_x	Local Reynolds number
c_1, c_2	Concentration	Sh_x	Local Sherwood number
D_A, D_B	Brownian motion coefficient (m^2/s)	T	Temperature $K\left(^\circ C\right)$
f'	Dimensionless velocity	T_∞	Free-stream temperature $K\left(^\circ C\right)$
g	Dimensionless concentration	T_w	Variable temperature at the sheet
h_s	Heterogeneous reaction rate	u, v	Velocity components along x, y directions respectively (m/s)
K_s	Heterogeneous reaction's strength	x, y	Cartesian coordinate system (m)
K^*	Permeability of the porous medium	***Greek Symbols***	
K	Permeability parameter	θ	Dimensionless temperature
Kc	Chemical reaction parameter	ρ_f	Density of base fluid (kg/m^3)
Kc^*	Homogeneous reaction rate	ρ_{nf}	Density of nanofluid (kg/m^3)
k_f	Thermal conductivity of the base fluid (m^2/s)	ρ_s	Density of solid nanoparticle (kg/m^3)
k_{nf}	Thermal conductivity of the nanofluid (m^2/s)	ϑ_f	Kinematic viscosity of the base fluid (m^2/s)
k_s	Thermal conductivity of the solid nanoparticle (m^2/s)	ϑ_{nf}	Kinetic velocity of the hybrid nanofluid (m^2/s)
M	Magnetic Parameter	δ	Ratio of mass diffusion coefficient
Nu_x	Local Nusselt number	$(\rho c_p)_f$	Specific heat capacitance of the base fluid (J/kg K)
Pr	Prandtl number	$(\rho c_p)_{nf}$	Specific heat capacitance of the hybrid nanofluid (J/kg K)
Q	Exponential space-based heat source/sink parameter	μ_{nf}	Viscosity of the nanofluid (kg/ms)

exponentially elongating sheet. Nayak et al. [9] studied the mixed convection flow of third grade nanofluid over an inclined stretched Riga plate. Manjunatha et al. [10] analysed the peristaltic transport of Jeffery fluid through an inclined elastic tube with porous walls and slip boundary conditions.

To enhance the thermal conductivity of common fluids, such as water and ethylene glycol etc., nanoparticles (metals/metallic oxide) are mixed with a base fluid to enhance the thermal transport of the nanofluid, which increases the rate of heat transfer. Choi [11] was first invented nanofluid. Buongiorno [12] conducted detailed investigation on convective transport in nanoliquids. He found that the Brownian moment and thermophoresis mechanisms are very significant factors in such advancement in the thermal conductivity of nanoliquids. He also developed a mathematical model to study the heat transport of nanoliquids. Das et al. [13] studied the flow of nanofluids over an unsteady stretching surface in presence of thermal radiation. Rudraswamy and Gireesha [14] explored the MHD nanofluid flow over an exponentially widening sheet. Nandkeolyar et al. [15] studied the effect of chemical reaction and heat absorption on MHD nanoliquid flow past an extending sheet. Hayat et al. [16] and

Mahanthesh et al. [17] have examined the flow over a non-linearly widening sheet. Nagaraja and Gireesha [18] investigated the convective flow of Casson fluid with exponential space-dependent heat generation. Bhattacharyya and Layek [19] studied flow of nanofluid over an exponentially stretching permeable sheet. Swain et al. [20] observed the thermal slip effect on MHD nanofluid convective flow over a vertical plate in a porous medium.

The present study is an extension work of Nandkeolyar et al. [15] by considering the influences of thermal radiation and exponential space-based heat source/sink in energy equation and porous matrix in momentum equation. The governing PDEs are converted into coupled non-linear ODEs by using suitable similarity solutions. The efficient shooting technique is applied to solve these ODEs. The effects of various operating parameters are shown through graphs and tables. The objective of the paper is to simulate the effect of important parameters such as transverse magnetic field, porous matrix, thermal radiation, and exponential space-based heat source/sink on flow, heat and mass transfer phenomena.

2. Formulation of the problem

Consider a steady two dimensional boundary layer flow of nanofluid over a stretching plate under the influence of thermal radiation and exponential space-based heat source/sink. Let us consider two chemically reacting foreign species A and B with concentrations c_1 and c_2 respectively. The plate is taken along x-axis and y-axis is taken normal to it. The transverse magnetic field of strength B_0 is applied along y-axis. The flow of fluid is restricted to $y > 0$. Let the velocity of the plate be $u_w(x)$ and the temperature at the surface is kept at $T_w(x)$. The flow geometry is depicted in Fig. 1. There is a homogeneous reaction takes place between the species A and B as [15]

$$A + 2B \to 3B, \text{rate} = Kc^* c_1 c_2^2 \tag{1}$$

whereas a heterogeneous first order, isothermal reaction undergo on the catalyst surface, as

$$A \to B, \text{rate} = h_s c_1 \tag{2}$$

where Kc^* and h_s are homogeneous and heterogeneous reaction rates respectively.

Under the above assumptions, the governing equations of the boundary layer flow of nanofluid following Nandkeolyar et al. [15] are given by

$$\frac{\partial u}{\partial x} + \frac{\partial v}{\partial y} = 0, \tag{3}$$

$$u\frac{\partial u}{\partial x} + v\frac{\partial u}{\partial y} = \upsilon_{nf}\frac{\partial^2 u}{\partial y^2} - \frac{\sigma_{nf} B_0^2 u}{\rho_{nf}} - \frac{\upsilon_{nf} u}{K^*}, \tag{4}$$

$$u\frac{\partial T}{\partial x} + v\frac{\partial T}{\partial y} = \frac{k_{nf}}{\left(\rho c_p\right)_{nf}}\frac{\partial^2 T}{\partial y^2} + \frac{16\sigma^* T_\infty^3}{3k^*\left(\rho c_p\right)_{nf}}\frac{\partial^2 T}{\partial y^2} + \frac{Q^*}{\left(\rho c_p\right)_{nf}}\left(T - T_\infty\right)\exp\left(-\sqrt{\frac{c}{\upsilon_f L}}ny\right), \tag{5}$$

$$u\frac{\partial c_1}{\partial x} + v\frac{\partial c_1}{\partial y} = D_A\frac{\partial^2 c_1}{\partial y^2} - Kc^* c_1 c_2^2, \tag{6}$$

$$u\frac{\partial c_2}{\partial x} + v\frac{\partial c_2}{\partial y} = D_B\frac{\partial^2 c_2}{\partial y^2} + Kc^* c_1 c_2^2, \tag{7}$$

with the corresponding boundary conditions as

$$u = u_w(x) = \frac{ax}{L}, v = 0, T = T_w = T_\infty + b\left(\frac{x}{L}\right)^2,$$
$$D_A\frac{\partial c_1}{\partial y} = h_s c_1, D_B\frac{\partial c_2}{\partial y} = -h_s c_1 \text{ at } y = 0 \tag{8}$$

$$u \to 0, T \to T_\infty, c_1 \to c_0, c_2 \to 0 \text{ at } y \to \infty. \tag{9}$$

The effective nanofluid properties are given by

$$\mu_{nf} = \frac{\mu_f}{(1-\phi)^{2.5}}, \rho_{nf} = (1-\phi)\rho_f + \phi\rho_s,$$
$$\left(\rho c_p\right)_{nf} = (1-\phi)\left(\rho c_p\right)_f + \phi\left(\rho c_p\right)_s,$$

$$\sigma_{nf} = \sigma_f \left[1 + \frac{3\left(\frac{\sigma_s}{\sigma_f} - 1\right)\phi}{\left(\frac{\sigma_s}{\sigma_f} + 2\right) - \left(\frac{\sigma_s}{\sigma_f} - 1\right)\phi} \right],$$

$$\frac{k_{nf}}{k_f} = \frac{2k_f + k_s - 2\phi\left(k_f - k_s\right)}{2k_f + k_s + \phi\left(k_f - k_s\right)},$$

where ϕ is the solid volume fraction, μ_f and μ_{nf} are the dynamic viscosities, υ_f and υ_{nf} are the kinematic viscosities, ρ_f and ρ_{nf} are the densities, $\left(\rho c_p\right)_f$ and $\left(\rho c_p\right)_{nf}$ are the heat capacitances, k_f and k_{nf} are the thermal conductivities and σ_f and σ_{nf} are the electrically conductivities of the base fluid and nanofluid respectively.

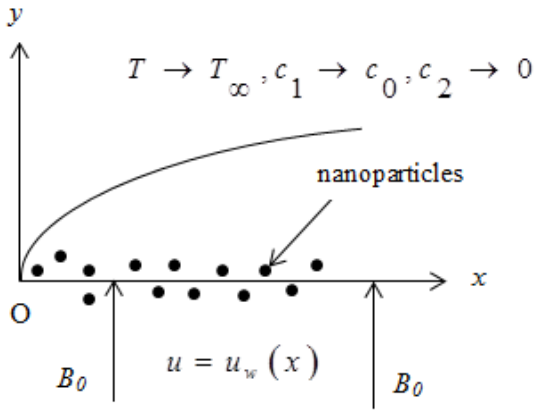

Fig. 1. Flow configuration

Let us introduce the stream function ψ such that $u = \frac{\partial \psi}{\partial y}$, $v = -\frac{\partial \psi}{\partial x}$ and similarity transformations

$$\psi = \sqrt{\frac{a\upsilon_f}{L}} x f(\eta), \eta = y\sqrt{\frac{a}{\upsilon_f L}},$$

$$\theta(\eta) = \frac{T - T_\infty}{T_w - T_\infty}, c_1 = a_0 \Phi(\eta), c_2 = a_0 h(\eta) \tag{10}$$

where η is the similarity variable and L is the characteristic length of the flow.
In view of equation (10), the equations (3) – (7) become

$$\zeta_1\zeta_2 f''' + ff'' - f'^2 - \zeta_2\left(\zeta_3 M + \zeta_1 K\right) f' = 0, \tag{11}$$

$$\zeta_4\left\{\frac{k_{nf}}{k_f} + \frac{4}{3}R\right\}\theta'' + Pr\left\{f\theta' + \zeta_4 Q\exp(-n\eta)\right\} = 0, \tag{12}$$

$$\Phi'' + Sc\left\{f\Phi' - Kc\Phi h^2\right\} = 0, \tag{13}$$

$$h'' + \frac{Sc}{\delta}\left\{fh' + Kc\Phi h^2\right\} = 0, \tag{14}$$

where $\zeta_1 = \frac{1}{(1-\phi)^{2.5}}, \zeta_2 = \frac{1}{(1-\phi) + \phi\left(\frac{\rho_s}{\rho_f}\right)}$,

$$\zeta_3 = 1 + \frac{3\left(\frac{\sigma_s}{\sigma_f} - 1\right)\phi}{\left(\frac{\sigma_s}{\sigma_f} + 2\right) - \left(\frac{\sigma_s}{\sigma_f} - 1\right)\phi},$$

$$\zeta_4 = \frac{1}{(1-\phi) + \phi\frac{\left(\rho c_p\right)_s}{\left(\rho c_p\right)_f}},$$

$$M = \frac{\sigma_f B_0^2 L}{a\rho_f}, K = \frac{\upsilon_f L}{aK^*}, R = \frac{4\sigma^* T_\infty^3}{k_f k^*}, \delta = \frac{D_B}{D_A},$$

$$\mathrm{Pr} = \frac{\upsilon_f\left(\rho c_p\right)_f}{k_f}, Q = \frac{2LQ^*}{a\left(\rho c_p\right)_f}, Sc = \frac{\upsilon_f}{D_A}.$$

The non-dimensional form of boundary conditions (8) and (9) are

$$f(\eta) = 0, f'(\eta) = 1, \theta(\eta) = 1, \Phi'(\eta) = K_s\Phi, \delta h' = -K_s\Phi \quad \text{at } \eta = 0, \tag{15}$$

$$f'(\eta) \to 0, \theta(\eta) \to 0, \Phi(\eta) \to 1, h(\eta) \to 0 \quad \text{as } \eta \to \infty. \tag{16}$$

Here $K_s = \frac{h_s}{D_A}\sqrt{\frac{\upsilon_f L}{c}}$ measures the heterogeneous reaction's strength.
Assuming that the chemical species A and B have equal diffusivity i.e. $\delta = 1$ [21], we get

$$\Phi(\eta) + h(\eta) = 1 \tag{17}$$

Therefore, equations (13) and (14) reduce to

$$\Phi'' + Sc\left\{ f\Phi' - Kc\Phi\left(1-\Phi\right)^2 \right\} = 0 \quad (18)$$

Subject to conditions

$$\Phi'(\eta) = K_s\Phi(\eta) \text{ at } \eta = 0,$$

$$\Phi(\eta) \to 1 \text{ as } \eta \to \infty \quad (19)$$

The local skin friction coefficient and Nusselt number are given by

$$C_f\sqrt{\mathrm{Re}_x} = \frac{1}{(1-\phi)^{2.5}} f''(0),$$

$$\frac{Nu_x}{\sqrt{\mathrm{Re}_x}} = -\left(\frac{k_{nf}}{k_f} + \frac{4}{3}R\right)\theta'(0).$$

Table 1: Thermophysical properties of H_2O, Cu and Al_2O_3 [22]

Property	H_2O	Cu	Al_2O_3
$\rho\left(\mathrm{kg\,m^{-3}}\right)$	997.1	8933	3970
$c_p\left(\mathrm{J\,kg^{-1}K^{-1}}\right)$	4179	385	765
$k\left(\mathrm{W\,m^{-1}\,K^{-1}}\right)$	0.613	401	40
$\sigma\times10^{-6}\left(\mathrm{S\,m^{-1}}\right)$	5.5×10^{-12}	59.6	36.9

3. Results and discussion

The dimensionless coupled nonlinear ODEs are solved numerically by effective shooting technique using MATLAB software to observe the influences of the related operating parameters on velocity, temperature, concentration as well as force coefficient and rate transfer coefficient. Table 1 provides the properties of water and nanoparticles at 25^0C. The impacts of such parameters are depicted graphically in Figs. 2-11 and Table 3. During numerical simulations the values of the parameters are fixed as $M = Kc = 0.5$, $K = 0.3, \phi = 0.01, \mathrm{Pr} = 6.2, R = K_s = Q_e = 0.1$, $n = 2, Sc = 1$. A comparison is made with previously published works of Gorla and Sidawi [23], Khan and pop [24] and Devi and Devi [25] as shown in Table 1. It is found that our numerical results are in very good agreement.

Fig. 2 depicts the effect of volume fraction of nanoparticles on velocity distribution $f'(\eta)$. It is seen that $f'(\eta)$ increases due to the absence of surface tension forces and therefore, the momentum boundary layer thickness increases. The same observation was made by Sravan Kumar and Rushi Kumar [26] and Nandkeolyar et al. [15]. Fig. 3 portrays that the velocity profiles for the various magnetic parameter. It is observed that an increase in magnetic parameter the velocity decreases. It is due to the fact that the application of transverse magnetic field will result in a Lorentz force similar to drag force, which tends to resist the fluid flow and thus reducing its velocity and it is also noticed that the momentum boundary layer thickness increases with increasing value of the magnetic parameter. Physically it is seen that when any fluid is subjected to a magnetic field than the viscosity rises. The results of which is that the fluid's capacity to transfer force can be restricted with help of an electromagnet which gives rise to its various possible control-based applications including MHD ion propulsion, electromagnetic tossing of meats, MHD control time etc. Fig. 4 shows the effect of porosity parameter(K) on $f'(\eta)$. The velocity of both nanofluids decreases with increase in K. This is due to Darcy resistance caused by the porous matrix. Moreover, the $Al_2O_3 - water$ nanofluid is of lower velocity than the $Cu - water$ nanofluid.

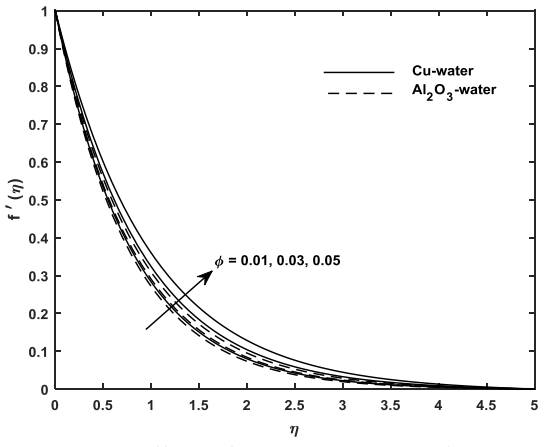

Fig. 2 Effect of ϕ on velocity profiles

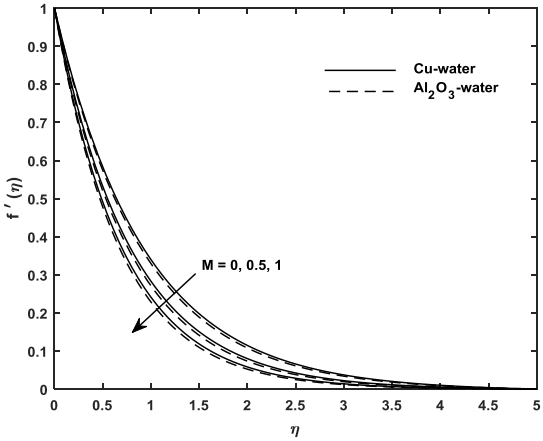

Fig. 3 Effect of M on velocity profiles

Fig. 5 displays the impact of radiation parameter (R) and Prandtl number $(\Pr)$ on temperature distribution $\theta(\eta)$. It is observed that $\theta(\eta)$ decreases with increase in $\Pr$. Since $\Pr$ is the ratio of momentum diffusivity to thermal diffusivity, consequently, larger values of $\Pr$ increases the thickness of the boundary layer, which increases the cooling efficiency of the nanomaterial. Fluids having lowest $\Pr$ have good thermal conductivities; therefore, thick boundary layer structures are maintained for diffusing heat. Further, higher values of radiation parameter boost the temperature profiles uniformly in the entire flow domain. Since the increase in thermal radiation provides more heat to the nanofluid which causes the increase in temperature and thermal boundary layer thickness.

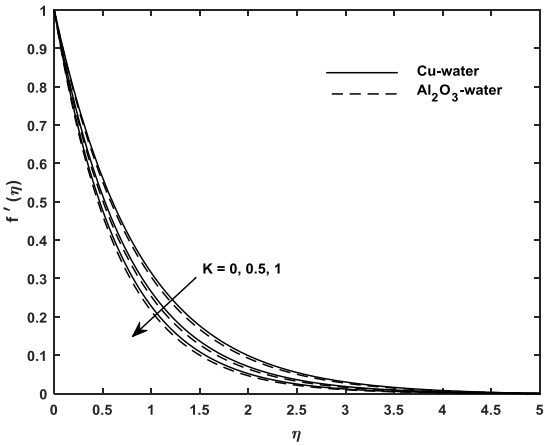

Fig. 4 Effect of K on velocity profiles

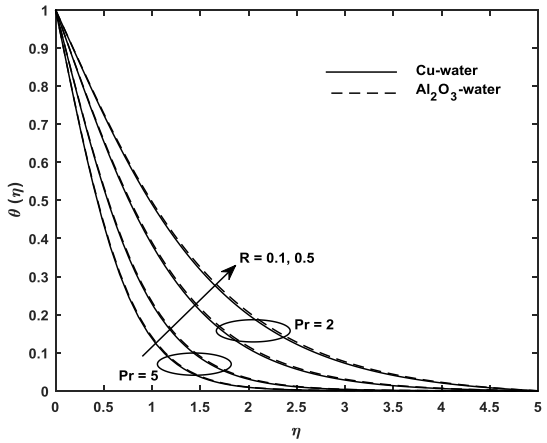

Fig. 5 Effects of $\Pr$ and R on temperature profiles

Fig. 6 shows the effect of volume fraction of nanoparticles of the temperature distribution. It is perceived that with the increasing volume fraction of nanoparticles the thermal boundary layer increases. Further, oxide nanoparticles have much higher heat conductivity than metallic nanoparticles. Fig. 7 displays the influence of exponential space-based heat source/sink (ESHS) parameter on temperature profiles. It is noted that increases with increasing values of. This is because the ESHS process supplies heat in the fluid, which consequently leads to a stronger the thermal boundary layer. Fig. 8 indicates that $\theta(\eta)$ is a decreasing function of n. Moreover, the $Al_2O_3 - water$ nanofluid is of higher temperature than the $Cu - water$ nanofluid.

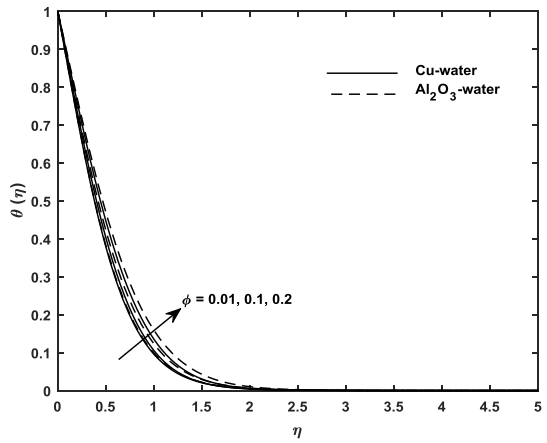

Fig. 6 Effect of ϕ on temperature profiles

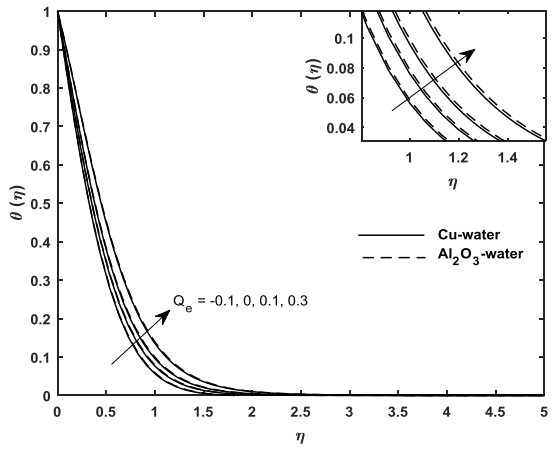

Fig. 7 Effect of Q_e on temperature profiles

Fig. 9 shows the effect of nanoparticle volume fraction on concentration distribution $\Phi(\eta)$. It is seen that nanoparticle volume fraction increases the concentration profiles. Figs. 10 and 11 represent the effects of homogeneous reaction rate (Kc) and heterogeneous reaction rate (K_s) on $\Phi(\eta)$ respectively. It is seen that both parameters decreases $\Phi(\eta)$. Further, heterogeneous reaction has a stronger effect on species concentration than the homogeneous reaction. Moreover, the $Al_2O_3 - water$ nanofluid is of lower concentration than the $Cu - water$ nanofluid.

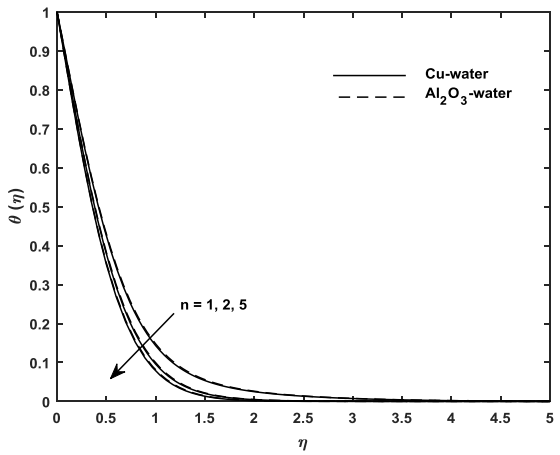

Fig. 8 Effect of n on temperature profiles

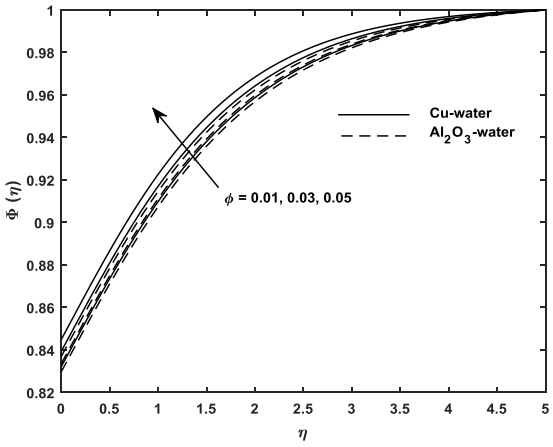

Fig. 9 Effect of ϕ on concentration profiles

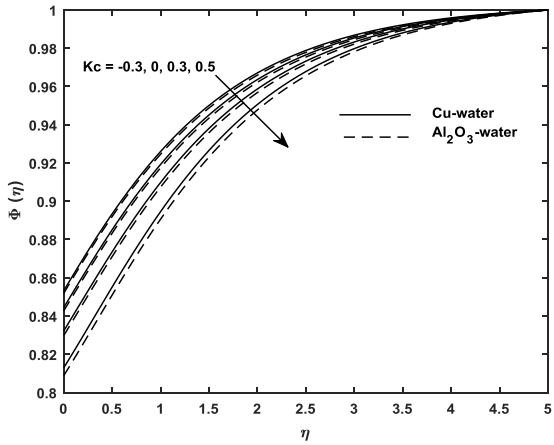

Fig. 10 Effect of Kc on concentration profiles

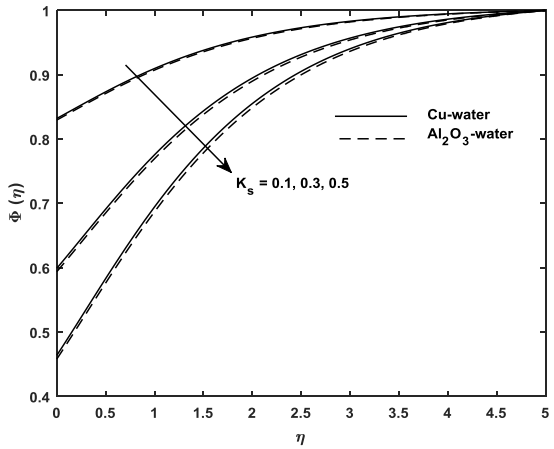

Fig. 11 Effect of K_S on concentration profiles

Table 3 shows the behaviour of physical quantities of interest viz. skin friction

coefficient and local Nusselt number by the influences of pertinent parameters such as ϕ, M, R, n and Q_e. It is observed that skin friction coefficient $-f''(0)$ is increases with an increase in M and deceases with ϕ. Further, it is seen that $-f''(0)$ is higher for $Al_2O_3 - water$ nanofluid than that of $Cu - water$ nanofluid. The local Nusselt number is getting enhanced on increasing of ϕ, R and n whilst decreases with M and Q_e.

4. Conclusions

From the present study the major finding are:

- Skin friction coefficient increases with an increase in M and deceases with ϕ.
- The higher values of ϕ enhance the velocity, temperature and concentration profiles.
- Temperature profile increases with in R and Q_e but decreases with Pr and n.
- Velocity of $Al_2O_3 - water$ nanofluid is slightly on lower side as compared to $Cu - water$ nanofluid whereas reverse effect is observed in case of temperature profile.

International Journal of Thermofluid Science and Technology (2021)
Volume 8, Issue 3, Paper No. 080302
https://doi.org/10.36963/IJTST.2021080302
Research Article

Table 3: Computation of $-f''(0)$ and $-\theta'(0)$ when $K = 0.5, \Pr = 6.2, K_S = Kc = 0.1, Sc = 1$.

ϕ	M	R	n	Q_e	$Cu-water$		$Al_2O_3-water$	
					$-f''(0)$	$-\theta'(0)$	$-f''(0)$	$-\theta'(0)$
0.01	0.1	0.1	1	0.1	1.22149	1.48887	1.26154	1.47513
0.05	0.1	0.1	1	0.1	1.10139	1.63098	1.25667	1.57325
0.05	0.5	0.1	1	0.1	1.21713	1.59518	1.40621	1.52708
0.05	1	0.1	1	0.1	1.34822	1.55453	1.57343	1.47551
0.05	1	0.5	1	0.1	1.34822	1.81234	1.57343	1.70986
0.05	1	1	1	0.1	1.34822	2.06569	1.57343	1.93582
0.05	1	1	2	0.1	1.34822	2.24505	1.57343	2.12484
0.05	1	1	5	0.1	1.34822	2.37365	1.57343	2.25749
0.05	1	1	5	0.3	1.34822	2.15960	1.57343	2.04150
0.05	1	1	5	0.5	1.34822	1.94556	1.57343	1.82551
0.05	1	1	5	-0.1	1.34822	2.58769	1.57343	2.47348

- Both homogeneous and heterogeneous reaction parameters decline the species concentration inside the boundary layer region.
- The rate of heat transfer increases with an increase in ϕ, R and n while decreases with M and Q_e.

References

[1] S. Nadeem, R. U. I. Haq, Z. H. Khan, Numerical solution of non-Newtonian nanofluid flow over a stretching sheet. Appl. Nanosci. 4 (2014) 4625-4631.

[2] B. J. Gireesha, B. Mahanthesh, M. M. Rashidi, MHD boundary layer heat and mass transfer of a chemically reacting Casson fluid over a permeable stretching surface with non-uniform heat source/sink. Int. J. Industrial Mathematics. 7 (2015) 247-260.

[3] K. Das, Nanofluid flow over a non-linear permeable stretching sheet with partial slip. Journal of the Egyptian Mathematical Society. 23 (2015) 451-456.

[4] U. Farooq, T. Hayat, A. Alsaedi, S. J. Liao, Series solutions of non-similarity boundary layer flows of nano-fluids over stretching surfaces. Numer Algor. 70 (2015) 43-59.

[5] B. C. Rout, S. R. Mishra, Thermal energy transport on MHD nanofluid flow over a stretching surface: A comparative study. Engineering Science and Technology, an International Journal. 21 (2018) 60-69.

[6] K. Swain, S. K. Parida, G. C. Dash, MHD flow of viscoelastic nanofluid over a stretching sheet in a porous medium with heat source and chemical reaction. Annales de Chimie- Science des Matériaux. 42 (2018) 7-21.

[7] B. Shankar Goud, B. Suresh Babu, M. N Raja Shekar, G. Srinivas, Mass Transfer Effects on MHD Flow through Porous Medium past an Exponentially Accelerated Inclined Plate with Variable Temperature and Thermal Radiation, International Journal of Thermofluid Science and Technology. 6 (2019) Paper No. 19060402.

[8] M. Senapati, K. Swain, S. K. Parida, Numerical analysis of three-dimensional MHD flow of Casson nanofluid past an exponentially stretching sheet. Karbala International Journal of Modern Science. 6 (2020) Article 13.

[9] M. K. Nayak, A. K. Abdul Hakeem, B. Ganga, Influence of non-uniform heat source/sink and variable viscosity on mixed convection flow of third grade

*Corresponding e-mail: kharabela1983@gmail.com (Kharabela Swain)

nanofluid over an inclined stretched Riga plate, International Journal of Thermofluid Science and Technology. 6 (2019) Paper No. 19060401.

[10] G. Manjunatha, C. Rajashekhar, Hanumesh Vaidya, K. V. Prasad, Saraswati, B. B. Divya, Heat Transfer Analysis on Peristaltic Transport of a Jeffery Fluid in an Inclined Elastic Tube with Porous Walls, International Journal of Thermofluid Science and Technology. 7 (2020) Paper No. 20070101.

[11] S. U. S. Choi, Enhancing thermal conductivity of the fluids with nanoparticles. ASME Fluids Eng. Division. 231 (1995) 99-105.

[12] J. Buongiorno, Convective transport in nanofluids. ASME J. Heat Transfer. 128 (2006) 240-250.

[13] K. Das, P. R. Duari, P. K. Kundu, Nanofluid flow over an unsteady stretching surface in presence of thermal radiation. Alexandria Engineering Journal. 53 (2014) 737-745.

[14] N. G. Rudraswamy, B. J. Gireesha, Influence of Chemical Reaction and Thermal Radiation on MHD Boundary Layer Flow and Heat Transfer of a Nanofluid over an Exponentially Stretching Sheet. Journal of Applied Mathematics and Physics. 2 (2014) 24-32.

[15] R. Nandkeolyar, B. K. Mahatha, G. K. Mahato, P. Sibanda, Effect of Chemical Reaction and Heat Absorption on MHD Nanoliquid Flow Past a Stretching Sheet in the Presence of a Transverse Magnetic Field. Magnetochemistry. 4 (2018) 18.

[16] T. Hayat, M. Imtiaz, A. Alsaedi, R. Mansoor, MHD flow of nanofluids over an exponentially stretching sheet in a porous medium with convective boundary conditions. Chin. Phys. B. 23 (2014) 054701.

[17] B. Mahanthesh, B. J. Gireesha, R. S. R. Gorla, Nonlinear radiative heat transfer in MHD three dimensional flow of water based nanofluid over a non-linearly stretching sheet with convective boundary condition. Journal of the Nigerian Mathematical Society. 35 (2016) 178-198.

[18] B. Nagaraja, B. J. Gireesha, Exponential space-dependent heat generation impact on MHD convective flow of Casson fluid over a curved stretching sheet with chemical reaction. Journal of Thermal Analysis and Calorimetry. (2020) doi.org/10.1007/s10973-020-09360-0.

[19] K. Bhattacharyya, G. C. Layek, Magnetohydrodynamic Boundary Layer Flow of Nanofluid over an Exponentially Stretching Permeable Sheet. Physics Research International. (2014) doi.org/10.1155/2014/592536.

[20] K. Swain, S. K. Parida, G. C. Dash, Thermal slip effect is MHD nanofluid convective flow over a vertical plate embedded in a porous medium. European Journal of Electrical Engineering. 20 (2018) 215-233.

[21] F. Almutairi, S. M. Khaled, A. Ebaid, MHD Flow of Nanofluid with Homogeneous-Heterogeneous Reactions in a Porous Medium under the Influence of Second-Order Velocity Slip. Mathematics. 7 (2019) 220.

[22] A. Mahdy, Impacts of homogeneous-heterogeneous chemical reactions and inclined magnetic field on unsteady nanofluids flow. AIP Advances. 8 (2018) 115109.

[23] R. S. R. Gorla, I. Sidawi, Free convection on a vertical stretching surface with suction and blowing. Appl. Sci. Res. 52 (1994) 247-257.

[24] W. A. Khan, I. Pop, Boundary-layer flow of a nanofluid past a stretching sheet. International Journal of Heat and Mass Transfer. 53 (2010) 2477-2483.

[25] S. S. U. Devi, S. P. A. Devi, Heat transfer enhancement of Cu−Al2O3/water hybrid nanofluid flow over a stretching sheet. J. Niger. Math. Soc. 36 (2017) 419-433.

[26] T. Sravan Kumar, B. Rushi Kumar, A comparative study of thermal radiation effects on MHD flow of nanofluids and heat transfer over a stretching sheet. Frontiers in Heat and Mass Transfer. 9 (2017) 13.